

Cluster Synchronization of Networks via a Canonical Transformation for Simultaneous Block Diagonalization of Matrices

Shirin Panahi,¹ Isaac Klickstein,¹ and Francesco Sorrentino^{1, a)}

Mechanical Engineering Department, University of New Mexico, Albuquerque, NM 87131

We study cluster synchronization of networks and propose a canonical transformation for simultaneous block diagonalization of matrices that we use to analyze stability of the cluster synchronous solution. Our approach has several advantages as it allows us to: (1) decouple the stability problem into subproblems of minimal dimensionality while preserving physically meaningful information; (2) study stability of both orbital and equitable partitions of the network nodes and (3) obtain a parametrization of the problem in a small number of parameters. For the last point, we show how the canonical transformation decouples the problem into blocks that preserve key physical properties of the original system. We also apply our proposed algorithm to analyze several real networks of interest, and we find that it runs faster than alternative algorithms from the literature.

Keywords: Dynamical Network; Simultaneous Block Diagonalization ; Cluster Synchronization.

^{a)}Electronic mail: fsorrent@unm.edu

The problem of cluster synchronization of networks has been studied in a number of papers in the literature, see e.g.,^{22,27,29,32}, among others. This paper follows up on these previous studies and proposes a canonical simultaneous block diagonalization routine to decouple the stability problem into subproblems ('blocks') of minimal dimensionality. Our approach has mainly two advantages: (i) each block in which the original problem is decoupled has a clear physical interpretation and (ii) it is faster than other algorithms proposed in the literature when applied to the analysis of real network topologies. It also nicely reconnects with previous work^{22,27,29} as the results in our paper are found to coincide with those in these other papers, though the techniques used to decouple the stability problem are different.

I. INTRODUCTION

Cluster synchronization (CS) in networks of coupled oscillators has been the subject of vast research efforts, see e.g.,^{3,5,7,10,20,23,26,28,31}. This occurs when the network nodes are divided into clusters such that the nodes in each cluster synchronize on the same time evolution but these time evolutions are different for nodes in different clusters. Recent work^{20,22} has elucidated the relation between the symmetries of the network topology and the formation of clusters of synchronized dynamical units in the network. Reference²² analyzed the formation and stability of synchronized clusters that correspond to the orbits of the network symmetry group. References^{27,29,32} extended this study to the more general case of equitable clusters, where the nodes in each cluster are not necessarily symmetric, but receive the same total input from the nodes in each one of the clusters. Cluster synchronization in directed networks was recently addressed in¹⁴.

The master stability function (MSF) approach²¹ has been successfully applied to characterize stability of the complete synchronous solution for networks of coupled systems with Laplacian connectivity. The approach is based on decoupling the stability problem into a number of lower-dimensional problems, where each of the lower-dimensional problems depends on an eigenvalue p_i of the Laplacian matrix. The main advantage of this approach is that stability of the lower-dimensional system can be parametrized in a generic parameter p and one can determine the range R of the parameter p over which the master stability

function $\mathcal{M}(p) < 0$. Then stability can be directly assessed, *for any network* of interest, by verifying that the relevant eigenvalues p_i belong to the range R , i.e., $p_i \in R$. There are, therefore, two main components of this approach: the first one is the dimensionality reduction and the second one is the parametrization.

The case of cluster synchronization (CS) with non-Laplacian connectivity is more complex. In what follows, we will: (i) reduce the dimensionality of the problem and (ii) obtain a parametrization of the lower dimensional problem in a minimal number of parameters. The novelty of our work lies especially in point (ii). We will see that for the case of CS we can generate a ‘canonical transformation’ of the stability problem that corresponds to a minimal number of parameters.

II. PROBLEM DEFINITION: CLUSTER SYNCHRONIZATION

A network of coupled dynamical systems can be described by the following set of equations,

$$\dot{\mathbf{x}}_i(t) = \mathbf{F}(\mathbf{x}_i(t)) + \sum_{j=1}^N A_{ij} \mathbf{H}(\mathbf{x}_j(t)) \quad i = 1, \dots, N \quad (1)$$

where $\mathbf{x}_i(t)$ represents the m -dimensional state vector of node i and $\mathbf{F} : R^m \rightarrow R^m$ describes the time evolution of each individual system located at node i . The adjacency matrix A describes the network connectivity, i.e., $A_{ij} = A_{ji} = 1$ if there is a connection between nodes i and j and $A_{ij} = A_{ji} = 0$ otherwise. The function $\mathbf{H} : R^m \rightarrow R^m$ is the node-to-node coupling function. We call $\mathcal{V} = \{1, \dots, N\}$ the set of the network nodes.

Definition 1. *Equitable cluster partition.* *Given the adjacency matrix A , representing the network topology, one can partition the set of the network nodes \mathcal{V} into subsets that we call equitable clusters, $\mathcal{C}_1, \mathcal{C}_2, \dots, \mathcal{C}_C$, $\cup_{k=1}^C \mathcal{C}_k = \mathcal{V}$, $\mathcal{C}_k \cap \mathcal{C}_\ell = \emptyset$ for $k \neq \ell$, where*

$$\sum_{h \in \mathcal{C}_\ell} A_{ih} = \sum_{h \in \mathcal{C}_\ell} A_{jh}, \quad \forall i, j \in \mathcal{C}_k \quad (2)$$

$$\forall \mathcal{C}_k, \mathcal{C}_\ell \subset \mathcal{V}.$$

We call $|\mathcal{C}_k| = n_k$ the number of nodes in cluster $k = 1, \dots, C$, $\sum_{k=1}^C n_k = N$.

In order to find the equitable clusters, we apply the algorithm developed by Belykh and Hasler² to the network with adjacency matrix A . The algorithm returns a set of C equitable clusters $\mathcal{C}_1, \mathcal{C}_2, \dots, \mathcal{C}_C$. Information about each equitable cluster is contained in the $N \times N$

diagonal indicator matrix $E_k = \{E_{kij}\}$, $k = 1, \dots, C$, where the entry (i, i) of the matrix E_k is equal to 1 if node i is in cluster \mathcal{C}_k and is equal to 0 otherwise.

Definition 2. Colored Network. *The previously defined equitable clusters induce a colored network, where each node i is assigned a color k if node i is in cluster \mathcal{C}_k .*

Given an equitable partition of the network nodes, we can define an invariant subspace for the set of Eqs. (1), which we call the cluster synchronization manifold. The dynamics on this manifold is the flow-invariant cluster synchronous time evolution⁸ $\{\mathbf{s}_1(t), \mathbf{s}_2(t), \dots, \mathbf{s}_C(t)\}$, where $\mathbf{s}_1(t)$ is the synchronous solution for all nodes in cluster \mathcal{C}_1 , $\mathbf{s}_2(t)$ is the synchronous solution for nodes in cluster \mathcal{C}_2 , and so on.

The $C \times C$ quotient matrix Q is defined such that for each pair of equitable clusters \mathcal{C}_k and \mathcal{C}_l we have,

$$Q_{kl} = \sum_{j \in \mathcal{C}_l} A_{ij} \quad i \in \mathcal{C}_k. \quad (3)$$

The quotient matrix describes a network (the ‘quotient network’), for which all the nodes in each equitable cluster collapse to a single quotient node. By assuming the system of equations (1) evolves on the cluster synchronization manifold, and averaging over all the nodes in each cluster, we can derive the equations for the time evolution of the quotient network,

$$\dot{\mathbf{s}}_k(t) = \mathbf{F}(\mathbf{s}_k(t)) + \sum_{l=1}^C Q_{kl} \mathbf{H}(\mathbf{s}_l(t)), \quad k, l = 1, 2, \dots, C, \quad (4)$$

where the m -dimensional vector $\mathbf{s}_k(t)$ represents the state of the quotient network node $k = 1, \dots, C$.

Definition 3. Equitable clusters encoding matrix. *With knowledge of the clusters, we can construct the $N \times C$ equitable clusters encoding matrix O , such that $O_{ij} = 1$ if node i is in cluster \mathcal{C}_j and 0 otherwise for $i = 1, \dots, N$ and $j = 1, \dots, C$.*

Remark 1. *Given a network described by the adjacency matrix A and the equitable clusters encoding matrix O (see definition 3), the $C \times C$ -dimensional quotient matrix Q can be computed as follows²⁶,*

$$Q = (O^T O)^{-1} O^T A O. \quad (5)$$

To investigate the stability of the cluster synchronous solution, we consider a small perturbation $\delta\mathbf{x}_i = (\mathbf{x}_i - \mathbf{s}_k)$, $i \in \mathcal{C}_k$. By linearizing Eq. (1) about Eq. (4) we obtain the vectorial equation,

$$\delta\dot{\mathbf{x}}(t) = \left[\sum_{c=1}^{\mathcal{C}} E_c \otimes D\mathbf{F}(\mathbf{s}_c(t)) + \sum_{c=1}^{\mathcal{C}} AE_c \otimes D\mathbf{H}(\mathbf{s}_c(t)) \right] \delta\mathbf{x}(t), \quad (6)$$

in the mN - dimensional vector $\delta\mathbf{x}(t) = [\delta\mathbf{x}_1^T(t), \delta\mathbf{x}_2^T(t), \dots, \delta\mathbf{x}_N^T(t)]^T$. We are interested in the possibility that the stability problem for the mN -dimensional system Eq. (6) can be decoupled into a set of lower-dimensional equations. To this end, we will show how to obtain a transformation matrix T that block-diagonalizes the matrices AE_c while leaving the matrices E_c unchanged.

III. DIMENSIONALITY REDUCTION OF THE CLUSTER SYNCHRONIZATION STABILITY PROBLEM

As mentioned in the previous section, our goal is to reduce the stability problem into a set of independent lower-dimensional equations instead of dealing with the high-dimensional problem, Eq. (6). Ref.²² has used a transformation based on the irreducible representations of the symmetry group to block-diagonalize the set of Eqs. (6) for the case of a network with symmetries. A limitation of this approach is that it is only applicable to the case of ‘orbital clusters’ (corresponding to the orbits of the symmetry group, see e.g.³⁰) and not to the more general case of ‘equitable clusters’¹³. Stability of the cluster synchronous solution in the case of equitable clusters was first discussed in Refs.^{27,29}. An alternative method based on the approach of simultaneous block diagonalization of matrices (SBD)^{16–18}, firstly applied to the problem of complete synchronization of networks in⁹, was used for cluster synchronization in³². Different from³², in this paper we propose an SBD transformation that will lead to a ‘canonical SBD transformation’ of the stability problem. Our method applies to both the cases of equitable and orbital clusters. We will discuss the benefits of this canonical transformation in the rest of this paper.

The problem of simultaneous block diagonalization can be formalized as follows: given a set of $N \times N$ symmetric matrices $A^{(1)}, \dots, A^{(M)}$, find an $N \times N$ orthogonal matrix T such that the matrices $T^{-1}A^{(k)}T$ have a common block-diagonal structure for $k = 1, \dots, M$. It should be noted that such a block-diagonal structure is not unique in at least two senses:

first, the blocks may be permuted, resulting in block diagonal decompositions that are isomorphic; second, the matrices corresponding to certain blocks may be further refined into smaller blocks, resulting in a structures that are fundamentally different. A block diagonal structure with smaller blocks is considered to be finer; we are interested in the finest SBD as it provides the simplest elements in the decoupling of systems as described above.

In the rest of this paper, we will always focus on finding a finest SBD. We write

$$T = \mathcal{SBD}(A^{(1)}, A^{(2)}, \dots, A^{(M)}) \quad (7)$$

to indicate that the following transformation yields

$$T^{-1}A^{(k)}T = B^{(k)}, \quad k = 1, \dots, M, \quad (8)$$

where all the matrices $B^{(k)}$, $k = 1, \dots, M$ share the same finest block diagonal form,

$$B^{(k)} = \bigoplus_j B_j^{(k)}, \quad (9)$$

with the blocks $B_j^{(k)}$ all having the same sizes β_k for $k = 1, \dots, M$ and not being further reducible by a simultaneous transformation.

The method for calculating a finest SBD transformation proposed in¹⁸ requires two main steps: (i) Finding a matrix P that commutes with a set of matrices, and (ii) calculating the transformation matrix T formed of the eigenvectors of the matrix P .

A. Matrix P

In order to study stability of the cluster synchronization solution, we need to simultaneously block diagonalize the set of $C + 1$ matrices $\{A, E_1, E_2, \dots, E_C\}$ where the matrix A is the adjacency matrix of the network and each E_i is the binary and diagonal cluster indicator matrix³². Once we find $T = \mathcal{SBD}(A, E_1, E_2, \dots, E_C)$, the matrices A and E_i are transformed as follows,

$$T^{-1}AT = B = \bigoplus_{k=1}^r \hat{B}^k, \quad (10a)$$

$$T^{-1}E_iT = J_i = \bigoplus_{k=1}^r \hat{J}_i^k \quad i = 1, \dots, C, \quad (10b)$$

where B is the transformed matrix A , J_i is the transformed matrix E_i , and the blocks of the $C + 1$ -tuple $(\hat{B}^k, \hat{J}_1^k, \dots, \hat{J}_C^k)$ have the same dimensions β_k , $k = 1, \dots, r$, $\sum_{k=1}^r \beta_k = N$. In what follows, we will refer to $(\hat{B}^k, \hat{J}_1^k, \dots, \hat{J}_C^k)$ as a block tuple.

Without loss of generality, we assume that the network nodes are ordered so that the first n_1 nodes are the ones in cluster \mathcal{C}_1 , followed by the n_2 nodes in cluster \mathcal{C}_2 , and so on, and the last n_C nodes are the ones in cluster \mathcal{C}_C . Then the matrices E_k are in the following form,

$$E_1 = \begin{pmatrix} I_{n_1} & 0 \\ 0 & 0_{N-n_1} \end{pmatrix} \quad E_2 = \begin{pmatrix} 0_{n_1} & 0 & 0 \\ 0 & I_{n_2} & 0 \\ 0 & 0 & 0_{N-(n_1+n_2)} \end{pmatrix} \quad \dots \quad E_C = \begin{pmatrix} 0_{N-n_C} & 0 \\ 0 & I_{n_C} \end{pmatrix} \quad (11)$$

where I_{n_i} is the identity matrix of size n_i , and 0_{n_i} is the zero matrix of size n_i .

Lemma 1. *Any matrix P that commutes with the set of matrices E_i in Eq. (11) has the following block-diagonal structure,*

$$P = \begin{pmatrix} P_1 & 0 & \dots & 0 \\ 0 & P_2 & \dots & 0 \\ \vdots & \vdots & \ddots & \vdots \\ 0 & 0 & \dots & P_C \end{pmatrix} \quad (12)$$

where the block P_1 has dimension n_1 , the block P_2 has dimension n_2 , and so on.

Proof. The product PE_i must have columns of zeros in the same place as E_i , so if P is to commute with E_i then E_iP must also have these columns as zero. Because E_i has an identity block in its non-zero columns, this forces P to have zeros in the intersection rows where E_i has its identity block and the columns where E_i is zero. Placing all such zeros as necessary for each of the E_i gives the structure of P as claimed. \square

Following Lemma 1, we can see that the transformation matrix T , which has the eigenvectors of the matrix P for its columns, must also have the same block-diagonal structure as the matrix P ,

$$T = \begin{pmatrix} T_1 & 0 & \dots & 0 \\ 0 & T_2 & \dots & 0 \\ \vdots & \vdots & \ddots & \vdots \\ 0 & 0 & \dots & T_C \end{pmatrix} \quad (13)$$

where T_1 is the matrix of eigenvectors of P_1 , T_2 is the matrix of eigenvectors of P_2 , and so on.

Remark 2. A trivial consequence of Eq. (13) is that as the matrix T is orthogonal, each one of the block matrices T_k is also orthogonal, $T_k^T = T_k^{-1}$.

Remark 3. The particular block-diagonal structure of the matrix T , where each block T_k corresponds to cluster \mathcal{C}_k has important consequences. Each independent block obtained from application of the SBD transformation will only produce linear combinations of the states of nodes from the same cluster (same color). This implies that to each block corresponds a colored subnetwork (corresponding to the block), see Definition 2. It also follows that each block describes stability of either one cluster or a set of intertwined clusters^{22,27}.

Remark 4. An additional benefit of our matrix T is that each one of its rows is associated to one and only one of the clusters, in the sense that all the entries of that row that do not correspond to the nodes of that cluster are zero. This is important as it indicates the particular way in which the cluster is broken if the Lyapunov exponent of the corresponding block of the matrix B is positive²⁷, i.e., entries that are the same (different) correspond to nodes that remain (do not remain) synchronized after the breaking.

Lemma 2. Application of the block diagonal transformation matrix T to each cluster indicator matrix E_i ensures that $J_i = E_i$ for $i = 1, 2, \dots, C$. In other words, each E_i gets mapped back to itself using the transformation matrix T of Eq. (13).

Proof. By considering the matrices $\{E_1, E_2, \dots, E_C\}$ of Eq. (11) and the block diagonal transformation matrix T of Eq. (13) and by using the fact that a block-diagonal matrix can be inverted block by block, we have $T^{-1}E_iT = E_i$ for $i = 1, 2, \dots, C$. For instance, for E_1 we have:

$$T^{-1}E_1T = \begin{pmatrix} T_1^{-1} & 0 & \cdots & 0 \\ 0 & T_2^{-1} & \cdots & 0 \\ \vdots & \vdots & \ddots & \vdots \\ 0 & 0 & \cdots & T_C^{-1} \end{pmatrix} \begin{pmatrix} I_{n1} & 0 & \cdots & 0 \\ 0 & 0 & \cdots & 0 \\ \vdots & \vdots & \ddots & \vdots \\ 0 & 0 & \cdots & 0 \end{pmatrix} \begin{pmatrix} T_1 & 0 & \cdots & 0 \\ 0 & T_2 & \cdots & 0 \\ \vdots & \vdots & \ddots & \vdots \\ 0 & 0 & \cdots & T_C \end{pmatrix} = \begin{pmatrix} I_{c1} & 0 & \cdots & 0 \\ 0 & 0 & \cdots & 0 \\ \vdots & \vdots & \ddots & \vdots \\ 0 & 0 & \cdots & 0 \end{pmatrix} \quad (14)$$

□

Lemma 3. Each block T_i of the matrix T has a column with entries that are all the same.

Proof. According to Lemma 1 and Eq. (13), we know that both the matrices P and T are block-diagonal in C blocks, where each block corresponds to one cluster. Also, according to

Ref.²⁵ the adjacency matrix A corresponding to a network with C equitable clusters, has C ‘non-redundant’ eigenvectors \mathbf{v}_k , each one associated with a cluster \mathcal{C}_k , $k = 1, \dots, C$ whose entries \mathbf{v}_{ki} are all the same for $i \in \mathcal{C}_k$ and zero otherwise. From the facts that the matrix P commutes with A and has block-diagonal structure (Eq. (12)) it follows that the matrix P will also have eigenvectors \mathbf{v}_k , $k = 1, \dots, C$. Thus each block T_k associated with cluster \mathcal{C}_k has a column with entries that are all the same and equal to $n_k^{-1/2}$. \square

Remark 5. *The transformation matrix T has two properties in common with the transformation introduced in Refs.^{6,22}: one is the block diagonal structure (13) and the other one is the property (Lemma 3) that each block has a column with entries that are all the same. Thus the two transformations are similar, with the following differences: (1) the transformation matrix T is not based on calculation of the network symmetries and can be successfully applied to the case of equitable clusters and (2) the transformation matrix T is faster to compute.*

Lemma 4. *One of the block tuples resulting from the SBD transformation of the set $\{A, E_1, E_2, \dots, E_C\}$ is C -dimensional and corresponds to the quotient network dynamics.*

Proof. As the T matrix is orthogonal $T^{-1} = T^T$. From the matrix T^T it is possible to extract C rows, where each row $i = 1, \dots, C$ includes the column of the block T_i with entries that are all the same and equal to $n_i^{-1/2}$. We call Δ the matrix obtained by stacking together these C rows. We note that the so-constructed matrix $\Delta = (O^T O)^{-1/2} O^T$. Then the $C \times C$ -dimensional block,

$$\hat{B}^1 = \Delta A \Delta^T = (O^T O)^{1/2} Q (O^T O)^{-1/2}, \quad (15)$$

from which we see that the two matrices \hat{B}^1 and Q are similar. A similar proof can be found in¹².

\square

Remark 6. *Lemma 4 is useful as it allows us to identify one block-tuple that is associated with dynamics parallel to the cluster synchronization manifold (the dynamics of the quotient network.) We use the label $k = 1$ to indicate this block-tuple $(\hat{B}^1, \hat{J}_1^1, \dots, \hat{J}_C^1)$. We use the labels $k = 2, \dots, C$ to indicate the block-tuples associated with dynamics transverse to the synchronization manifold. The transverse block-tuples determine stability of the cluster synchronous solution²².*

Lemma 5. *The sub-matrices P_i $i = 1, 2, \dots, C$ can be found by computing the null subspace of the $\sum_i n_i^2 \times \sum_i n_i^2$ -dimensional matrix $S^T S$ defined below.*

Proof. By rewriting the adjacency matrix A as:

$$\begin{pmatrix} A_{11} & A_{12} & \cdots & A_{1C} \\ A_{21} & A_{22} & \cdots & A_{2C} \\ \vdots & \vdots & \ddots & \vdots \\ A_{C1} & A_{C2} & \cdots & A_{CC} \end{pmatrix} \quad (16)$$

the commutation equation $PA = AP$ becomes

$$\begin{pmatrix} P_1 & 0 & \cdots & 0 \\ 0 & P_2 & \cdots & 0 \\ \vdots & \vdots & \ddots & \vdots \\ 0 & 0 & \cdots & P_C \end{pmatrix} \begin{pmatrix} A_{11} & A_{12} & \cdots & A_{1C} \\ A_{21} & A_{22} & \cdots & A_{2C} \\ \vdots & \vdots & \ddots & \vdots \\ A_{C1} & A_{C2} & \cdots & A_{CC} \end{pmatrix} = \begin{pmatrix} A_{11} & A_{12} & \cdots & A_{1C} \\ A_{21} & A_{22} & \cdots & A_{2C} \\ \vdots & \vdots & \ddots & \vdots \\ A_{C1} & A_{C2} & \cdots & A_{CC} \end{pmatrix} \begin{pmatrix} P_1 & 0 & \cdots & 0 \\ 0 & P_2 & \cdots & 0 \\ \vdots & \vdots & \ddots & \vdots \\ 0 & 0 & \cdots & P_C \end{pmatrix} \quad (17a)$$

$$\begin{pmatrix} P_1 A_{11} & P_1 A_{12} & \cdots & P_1 A_{1C} \\ P_2 A_{21} & P_2 A_{22} & \cdots & P_2 A_{2C} \\ \vdots & \vdots & \ddots & \vdots \\ P_C A_{C1} & P_C A_{C2} & \cdots & P_C A_{CC} \end{pmatrix} = \begin{pmatrix} A_{11} P_1 & A_{12} P_2 & \cdots & A_{1C} P_C \\ A_{21} P_1 & A_{22} P_2 & \cdots & A_{2C} P_C \\ \vdots & \vdots & \ddots & \vdots \\ A_{C1} P_1 & A_{C2} P_2 & \cdots & A_{CC} P_C \end{pmatrix}. \quad (17b)$$

Equation (17b) corresponds to the following C^2 equations which should all be simultaneously solved:

$$P_i A_{ij} - A_{ij} P_j = 0_{n_i, n_j} \quad i, j = 1, 2, \dots, C \quad (18)$$

where n_i is the dimension of the sub-matrix P_i .

Define the function $\text{vec} : \mathbb{R}^{n \times m} \mapsto \mathbb{R}^{nm}$ that maps a matrix to a vector by stacking the columns of the matrix. We obtain the set of C^2 equations,

$$(A_{ij}^T \otimes I_{n_{pi}}) \text{vec}(P_i) - (I_{n_{pi}} \otimes A_{ij}) \text{vec}(P_j) = 0_{n_i, n_j} \quad (19)$$

Accordingly, Eq. (19) can be expressed as two linear systems of equations in the matrices,

$$S_1 = \begin{pmatrix} \bar{A}_1 & 0 & \cdots & 0 \\ 0 & \bar{A}_2 & \cdots & 0 \\ \vdots & \vdots & \ddots & \vdots \\ 0 & 0 & \cdots & \bar{A}_C \end{pmatrix} \quad (20a)$$

$$S_2 = \begin{pmatrix} A_{12}^T \otimes I_{n_1} & -I_{n_2} \otimes A_{12} & 0 & 0 \cdots & 0 & 0 \\ -I_{n_1} \otimes A_{21} & A_{21}^T \otimes I_{n_2} & 0 & 0 \cdots & 0 & 0 \\ A_{13}^T \otimes I_{n_1} & 0 & -I_{n_3} \otimes A_{13} & 0 \cdots & 0 & 0 \\ -I_{n_1} \otimes A_{31} & 0 & A_{31}^T \otimes I_{n_3} & 0 \cdots & 0 & 0 \\ \vdots & \vdots & \vdots & \vdots \ddots & \vdots & \vdots \\ A_{1C}^T \otimes I_{n_1} & 0 & 0 & 0 \cdots & 0 & -I_{n_C} \otimes A_{1C} \\ -I_{n_1} \otimes A_{C1} & 0 & 0 & 0 \cdots & 0 & A_{C1}^T \otimes I_{n_C} \\ 0 & A_{23}^T \otimes I_{n_2} & -I_{n_3} \otimes A_{23} & 0 \cdots & 0 & 0 \\ 0 & -I_{n_2} \otimes A_{32} & A_{32}^T \otimes I_{n_3} & 0 \cdots & 0 & 0 \\ \vdots & \vdots & \vdots & \vdots \ddots & \vdots & \vdots \\ 0 & A_{2C}^T \otimes I_{n_2} & 0 & 0 \cdots & 0 & -I_{n_C} \otimes A_{2C} \\ 0 & -I_{n_2} \otimes A_{C2} & 0 & 0 \cdots & 0 & A_{C2}^T \otimes I_{n_C} \\ \vdots & \vdots & \vdots & \vdots \ddots & \vdots & \vdots \\ 0 & 0 & 0 & 0 \cdots & A_{C-1,C}^T \otimes I_{n_{(C-1)}} & -I_{n_C} \otimes A_{C-1,C} \\ 0 & 0 & 0 & 0 \cdots & -I_{n_{(C-1)}} \otimes A_{C,C-1} & A_{C,C-1}^T \otimes I_{n_C} \end{pmatrix} \quad (20b)$$

where $\bar{A}_i = (A_{ii}^T \otimes I_{n_i}) - (I_{n_i} \otimes A_{ii})$. By stacking Eq. (20a) and (20b) together as $S = [S_1^T \ S_2^T]^T$, we search for a vector $\mathbf{p} = [\text{vec}(P_1)^T \ \text{vec}(P_2)^T \ \cdots \ \text{vec}(P_C)^T]^T$ that lies in $\mathcal{N}(S)$, the nullspace of S . The matrix $S \in \mathbb{R}^{N_r \times N_c}$ has number of rows $N_r = \sum_{i=1}^C \sum_{j=1}^C n_i n_j$ and number of columns $N_c = \sum_{i=1}^C n_i^2$. By using the property of nullspaces that $\mathcal{N}(S) = \mathcal{N}(S^T S)$, we instead look for a vector \mathbf{p} that lies in $\mathcal{N}(S^T S)$,

$$S^T S \mathbf{p} = \mathbf{0}_{N_c}, \quad (21)$$

where $S^T S \in \mathbb{R}^{N_c \times N_c}$. □

Remark 7. *It is worth mentioning that the original method¹⁸ requires finding a vector in the nullspace of a $N^2 \times N^2$ -dimensional matrix while the method derived here requires finding a vector in the nullspace of a $\sum_i n_i^2 \times \sum_i n_i^2$ -dimensional matrix where $\sum_i n_i^2$ is not greater than N^2 .*

$$n^2 = \left(\sum_i n_i \right)^2 \geq \sum_i n_i^2 \quad (22)$$

Equality only occurs if $C = 1$ while the minimum of $\sum_i n_i^2$ is achieved when $C = N$ (so $n_i = 1$).

By applying T to Eq. (6), we obtain,

$$\dot{\boldsymbol{\eta}}(t) = \left[(T^{-1} \sum_{k=1}^C E_k T) \otimes D\mathbf{F}(\mathbf{s}_k(t)) + (T^{-1} \sum_{k=1}^C A E_k T) \otimes D\mathbf{H}(\mathbf{s}_k(t)) \right] \boldsymbol{\eta}(t), \quad (23)$$

where $\boldsymbol{\eta}(t) = (T^{-1} \otimes I_m) \delta \mathbf{x}(t)$. Eq. (23) can be rewritten,

$$\dot{\boldsymbol{\eta}}(t) = \left[\sum_{k=1}^C J_k \otimes D\mathbf{F}(\mathbf{s}_k(t)) + \sum_{k=1}^C B J_k \otimes D\mathbf{H}(\mathbf{s}_k(t)) \right] \boldsymbol{\eta}(t), \quad (24)$$

which can be decoupled into r independent equations of smaller dimensions, in the blocks of the block diagonal matrices J_k and $B J_k$.

B. Importance of the canonical transformation

We call an SBD transformation of the set of $C+1$ matrices $\{A, E_1, E_2, \dots, E_C\}$ ‘*canonical*’ if the transformation maps the matrices E_1, E_2, \dots, E_C back to themselves. There are at least two main strengths of a canonical SBD transformation: (i) the parametrization associated with the SBD transformation, and (ii) the interpretation of the matrices resulting from this transformation. We briefly comment on both strengths below. Consider that the blocks obtained by the SBD transformation of the set of $C+1$ matrices $\{A, E_1, E_2, \dots, E_C\}$ have sizes β_k , $k = 1, \dots, r$, $\sum_{k=1}^r \beta_k = N$. Then the number of nonzero entries that parametrize the matrices after the transformation is equal to $p_1 = (C+1) \sum_{k=1}^r \beta_k (\beta_k + 1)/2$. In the case of a canonical SBD transformation the number of nonzero entries that parametrize the matrices after the transformation is equal to $p_2 = \sum_{k=1}^r \beta_k (\beta_k + 1)/2$, $p_2 < p_1$, taking into account that the matrices J_1, J_2, \dots, J_C are known ‘*a priori*’. Also in terms of interpretation, the diagonal matrices J_1, J_2, \dots, J_C with either zeros or ones on the main diagonal indicate that each network node after the transformation belongs to one and only one cluster, i.e., node i belongs (does not belong) to cluster k if the entry (i, i) of matrix J_k is one (zero). Therefore, one can still say that the resulting ‘nodes’ have a color (corresponding to the cluster they belong to) while node-node interactions are limited to the transformed matrix B , see also remarks 3 and 4. This is different from the case of a non-canonical transformation where the resulting ‘nodes’ do not necessarily have a color (i.e., they do not correspond to a single cluster of the original network) and there are in general $C+1$ ‘layers of connectivity’ between these nodes.

The SBD transformation described in Sec. III A is canonical while the SBD transformation proposed in³² is not. For example, consider the $N = 4$ -dimensional network with $C = 2$ clusters, shown in Fig. 1 (a). The nodes are colored according to the cluster to which they belong.

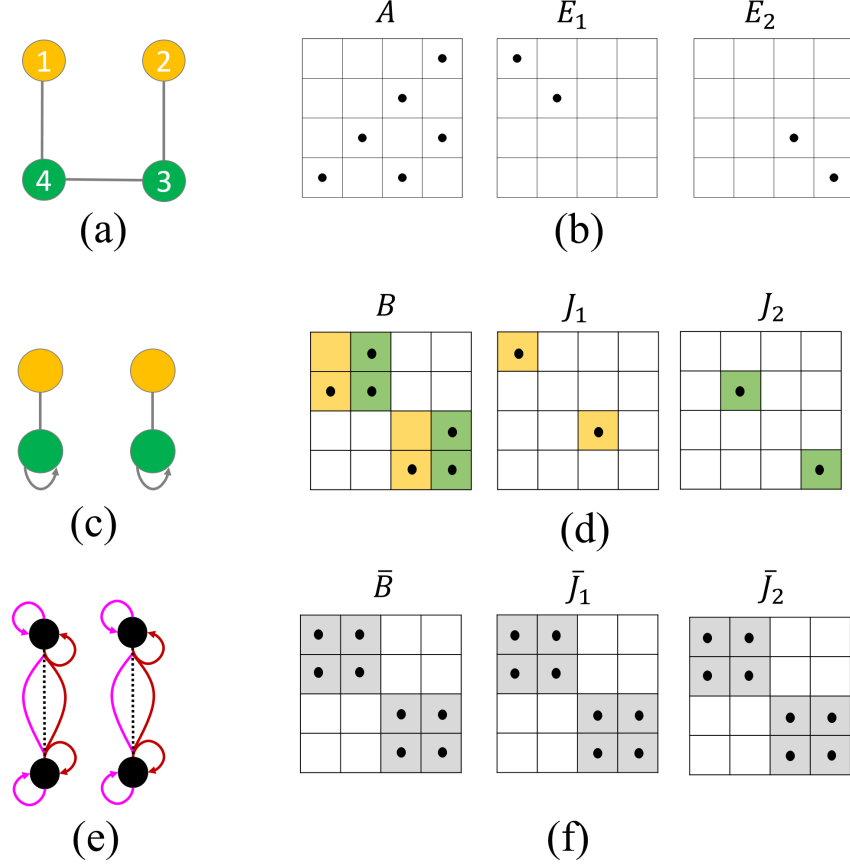


FIG. 1. (a) An $N = 4$ node network with $C = 2$ clusters. Nodes are color-coded according to the clusters to which they belong. (b) The adjacency matrix of the network (A) and the two cluster indicator matrices ((E_1, E_2)) are graphically shown, in which a nonzero entry is indicated as a black dot. (c) and (e) show the quotient and transverse sub-networks after application of the SBD transformation T and \tilde{T} , respectively. Subnetwork nodes are colored based on the cluster with which they are associated. Black nodes indicate that they are not associated with only one cluster. In (e) connections with different colors represent coupling through the \bar{B} subnetwork and the \bar{J}_i subnetworks. (d) The set of matrices $\{B, J_1, J_2\}$ and (f) the set of matrices $\{\bar{B}, \bar{J}_1, \bar{J}_2\}$ obtained by using the transformation T and \tilde{T} , respectively. The background color of each matrix entry indicates the cluster about which the dynamics is linearized. A gray background color indicates that the dynamics is linearized about multiple clusters.

Figure 1 shows the results after applying a canonical (c, d) and a non-canonical³² (e, f) SBD transformation. It can be seen that both transformations reduce the $4m$ -dimensional stability problem of Eq. (6) into a $2m$ -dimensional equation corresponding to the quotient

dynamics and a $2m$ -dimensional equation corresponding to the transverse dynamics. Only the latter is responsible for stability of the cluster synchronous solution. Equation (6) for the network of Fig. 1 is:

$$\begin{aligned} \delta\dot{\mathbf{X}} = \begin{pmatrix} \delta\dot{\mathbf{x}}_1 \\ \delta\dot{\mathbf{x}}_2 \\ \delta\dot{\mathbf{x}}_3 \\ \delta\dot{\mathbf{x}}_4 \end{pmatrix} &= \begin{pmatrix} D\mathbf{F}(\mathbf{s}_1) & 0 & 0 & 0 \\ 0 & D\mathbf{F}(\mathbf{s}_1) & 0 & 0 \\ 0 & 0 & D\mathbf{F}(\mathbf{s}_2) & 0 \\ 0 & 0 & 0 & D\mathbf{F}(\mathbf{s}_2) \end{pmatrix} \delta\mathbf{X} \\ &+ \begin{pmatrix} 0 & 0 & 0 & D\mathbf{H}(\mathbf{s}_2) \\ 0 & 0 & D\mathbf{H}(\mathbf{s}_2) & 0 \\ 0 & D\mathbf{H}(\mathbf{s}_1) & 0 & D\mathbf{H}(\mathbf{s}_2) \\ D\mathbf{H}(\mathbf{s}_1) & 0 & D\mathbf{H}(\mathbf{s}_2) & 0 \end{pmatrix} \delta\mathbf{X}. \end{aligned} \quad (25)$$

Using the canonical SBD transformation matrix T , Eq. (25) becomes,

$$\begin{aligned} \dot{\mathbf{Y}} = T^{-1}\delta\dot{\mathbf{X}} = \frac{\sqrt{2}}{2} \begin{pmatrix} \delta\dot{\mathbf{x}}_1 + \delta\dot{\mathbf{x}}_2 \\ -\delta\dot{\mathbf{x}}_3 - \delta\dot{\mathbf{x}}_4 \\ \delta\dot{\mathbf{x}}_1 - \delta\dot{\mathbf{x}}_2 \\ \delta\dot{\mathbf{x}}_3 - \delta\dot{\mathbf{x}}_4 \end{pmatrix} &= \begin{pmatrix} D\mathbf{F}(\mathbf{s}_1) & 0 & 0 & 0 \\ 0 & D\mathbf{F}(\mathbf{s}_2) & 0 & 0 \\ 0 & 0 & D\mathbf{F}(\mathbf{s}_1) & 0 \\ 0 & 0 & 0 & D\mathbf{F}(\mathbf{s}_2) \end{pmatrix} \mathbf{Y} \\ &+ \begin{pmatrix} 0 & -D\mathbf{H}(\mathbf{s}_2) & 0 & 0 \\ -D\mathbf{H}(\mathbf{s}_1) & D\mathbf{H}(\mathbf{s}_2) & 0 & 0 \\ 0 & 0 & 0 & D\mathbf{H}(\mathbf{s}_2) \\ 0 & 0 & D\mathbf{H}(\mathbf{s}_1) & -D\mathbf{H}(\mathbf{s}_2) \end{pmatrix} \mathbf{Y}, \end{aligned} \quad (26)$$

where the vectors $\mathbf{Y} = [\mathbf{Y}_1^T, \mathbf{Y}_2^T, \mathbf{Y}_3^T, \mathbf{Y}_4^T]^T$ in Eq. (26) is the transformed vector $\delta\mathbf{X}$ using canonical (T) transformation. We see that the dynamics of each transformed variable \mathbf{Y}_i is described by either one of the two Jacobians $D\mathbf{F}(\mathbf{s}_1)$ and $D\mathbf{F}(\mathbf{s}_2)$. This is due to the fact that the canonical transformation T only produces linear combinations of nodes belonging to the same cluster (see Remark 3.) For example, the yellow nodes in Fig. 1 (a) get mapped back to other yellow nodes in Fig. 1 (c), and so on. These transformed nodes are then coupled through the connections of only one network corresponding to the resulting matrix B (in two blocks.)

Using the non-canonical SBD transformation matrix \tilde{T} , Eq. (25) becomes,

$$\begin{aligned}
\dot{\mathbf{Z}} &= \tilde{T}^{-1} \delta \dot{\mathbf{X}} = \begin{pmatrix} -0.65\delta\dot{\mathbf{x}}_1 + 0.65\delta\dot{\mathbf{x}}_2 - 0.26\delta\dot{\mathbf{x}}_3 + 0.26\delta\dot{\mathbf{x}}_4 \\ -0.26\delta\dot{\mathbf{x}}_1 + 0.26\delta\dot{\mathbf{x}}_2 + 0.65\delta\dot{\mathbf{x}}_3 - 0.65\delta\dot{\mathbf{x}}_4 \\ 0.69\delta\dot{\mathbf{x}}_1 + 0.69\delta\dot{\mathbf{x}}_2 - 0.16\delta\dot{\mathbf{x}}_3 - 0.16\delta\dot{\mathbf{x}}_4 \\ 0.16\delta\dot{\mathbf{x}}_1 + 0.16\delta\dot{\mathbf{x}}_2 + 0.69\delta\dot{\mathbf{x}}_3 + 0.69\delta\dot{\mathbf{x}}_4 \end{pmatrix} \\
&= \begin{pmatrix} 0.14\mathbf{DF}(\mathbf{s}_1) + 0.86\mathbf{DF}(\mathbf{s}_2) & 0.35\mathbf{DF}(\mathbf{s}_1) - 0.35\mathbf{DF}(\mathbf{s}_2) & 0 & 0 \\ 0.35\mathbf{DF}(\mathbf{s}_1) - 0.35\mathbf{DF}(\mathbf{s}_2) & 0.86\mathbf{DF}(\mathbf{s}_1) + 0.14\mathbf{DF}(\mathbf{s}_2) & 0 & 0 \\ 0 & 0 & 0.05\mathbf{DF}(\mathbf{s}_1) + 0.95\mathbf{DF}(\mathbf{s}_2) & 0.22\mathbf{DF}(\mathbf{s}_1) - 0.22\mathbf{DF}(\mathbf{s}_2) \\ 0 & 0 & 0.22\mathbf{DF}(\mathbf{s}_1) - 0.22\mathbf{DF}(\mathbf{s}_2) & 0.95\mathbf{DF}(\mathbf{s}_1) + 0.05\mathbf{DF}(\mathbf{s}_2) \end{pmatrix} \\
&+ \begin{pmatrix} 0.35\mathbf{DH}(\mathbf{s}_1) - 0.51\mathbf{DH}(\mathbf{s}_2) & 0.86\mathbf{DH}(\mathbf{s}_1) + 0.20\mathbf{DH}(\mathbf{s}_2) & 0 & 0 \\ -0.14\mathbf{DH}(\mathbf{s}_1) + 1.2\mathbf{DH}(\mathbf{s}_2) & -0.35\mathbf{DH}(\mathbf{s}_1) - 0.49\mathbf{DH}(\mathbf{s}_2) & 0 & 0 \\ 0 & 0 & 0.22\mathbf{DH}(\mathbf{s}_1) + 1.17\mathbf{DH}(\mathbf{s}_2) & 0.95\mathbf{DH}(\mathbf{s}_1) - 0.05\mathbf{DH}(\mathbf{s}_2) \\ 0 & 0 & -0.05\mathbf{DH}(\mathbf{s}_1) + 0.72\mathbf{DH}(\mathbf{s}_2) & -0.22\mathbf{DH}(\mathbf{s}_1) + 0.95\mathbf{DH}(\mathbf{s}_2) \end{pmatrix} \quad (27)
\end{aligned}$$

where the vector $\mathbf{Z} = [\mathbf{Z}_1^T, \mathbf{Z}_2^T, \mathbf{Z}_3^T, \mathbf{Z}_4^T]^T$ in Eq. (27) is the transformed vector $\delta\mathbf{X}$ using the non-canonical (\tilde{T}) SBD transformation. We see that the transformation matrix \tilde{T} produces the same number of blocks with the same dimensions as the transformation matrix T . However, from Eq. (27) and Fig. 1 we see that application of the non-canonical SBD transformation does not preserve the color of the nodes in the original network. Also, we see that the individual \mathbf{Z}_i are coupled with one another through both the \mathbf{DF} and the \mathbf{DH} terms. This is shown in Fig. 1(e) where the resulting nodes are colored black to indicate that they do not correspond to any individual color of the original network. Connections of different colors are used to indicate the different types of coupling.

As has been stated before, the stability analysis of the cluster synchronization problem (Eq. (6)) is based on two main steps: the first one is the dimensionality reduction and the second one is the parametrization. Here, concerning the second step, we focus on the importance of a canonical SBD transformation in order to obtain a parametrization of the lower-dimensional problem in a minimal number of parameters. For example, consider the network from Ref.²² shown in Fig. 2 (a). We set $q_1 = A_{1,8} = A_{8,1}$ and $q_2 = A_{5,10} = A_{10,5}$ and parametrize the problem in terms of q_1 and q_2 . The two links between nodes 1 and 8 and nodes 5 and 10 are highlighted in yellow. Fig. 2 (b) and (c) show the block diagonal matrix B and \bar{B} obtained from application of the canonical (T) and non-canonical (\tilde{T}) transformation,

respectively. In both cases, we indicate with q_1 (q_2) the block entries that are affected by variations of the parameters q_1 (q_2 .) As we can see, changing q_1 and q_2 only affects a few entries of the block diagonal matrix in the case of the canonical transformation, but affects many more entries in the case of a non-canonical transformation. Looking at the transverse 2-dimensional block in (b) we see that q_1 only affects one entry of this block and q_2 only affects one other entry of that block. On the other hand, each entry of the 2-dimensional block in (c) is affected by both q_1 and q_2 .

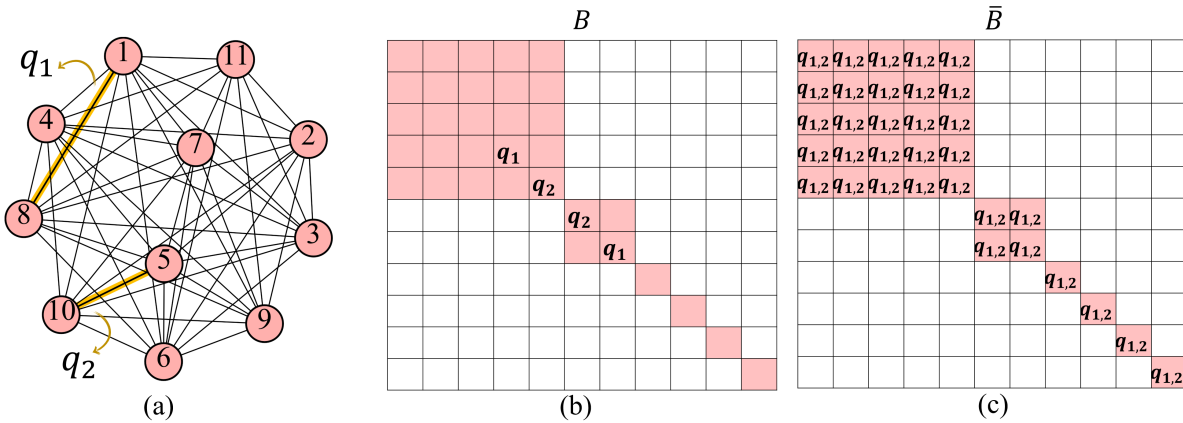


FIG. 2. (a) $N = 11$ -dimensional network from Ref.²² with two weighted edges. The two edges between nodes 1 and 8 and nodes 5 and 10 are highlighted in yellow. We set $q_1 = A_{1,8} = A_{8,1}$ and $q_2 = A_{5,10} = A_{10,5}$ and parametrize the problem in terms of q_1 and q_2 . (b) shows the matrix B obtained from application of a canonical SBD transformation and (c) shows the matrix \bar{B} obtained from application of a non-canonical SBD transformation. In both cases, we label with q_1 (q_2) the block entries that are affected by variations of the parameters q_1 (q_2 .)

IV. ORBITAL AND EQUITABLE PARTITIONS

We are now going to apply our approach to the case of a network for which the equitable and orbital clusters do not coincide. This network is from Ref.¹³. As for the other examples in this paper, the number and dimensions of the blocks will be the same as those obtained from the method in Ref.³² but the structure of the blocks will be different. We will comment on the benefits of using a canonical transformation.

We demonstrate the benefits of the canonical transformation with the $N = 8$ -dimensional

network from Ref.¹³ shown in Fig. 3 and 4. Figure 3 is for the case of the network equitable partition with $C = 2$ clusters and Fig. 4 is for the case of the network orbital partition with $C = 3$ clusters. We compare the results after application of the canonical SBD transformation T and the non-canonical SBD transformation \tilde{T} . Figure 3 shows that in both cases the SBD leads to a total of 5 blocks, one 2-dimensional block corresponding to the quotient network, one 3-dimensional block and three 1-dimensional blocks, all corresponding to the transverse dynamics.

An interesting case is that of the 3-dimensional block, which is shown in panels (c) for the case of the canonical transformation and (e) for the case of the non-canonical transformation. In panel (c) the dynamics of each node is linearized about the dynamics of one and only one of the quotient network nodes (and so it retains the color of that node), while in panel (e) each node is associated to a linear combination of the dynamics of the quotient network nodes. Also the nodes in (e) are coupled through different types of connections, consistent with the non-diagonal structure of the 3-dimensional blocks in (f).

Another example of a network for which the equitable and orbital clusters do not coincide from Ref.²⁷ is presented in the Supplementary Information. For this other example, for both the case of the orbital and equitable partition, we obtain the same decomposition in blocks already presented in Ref.²⁷.

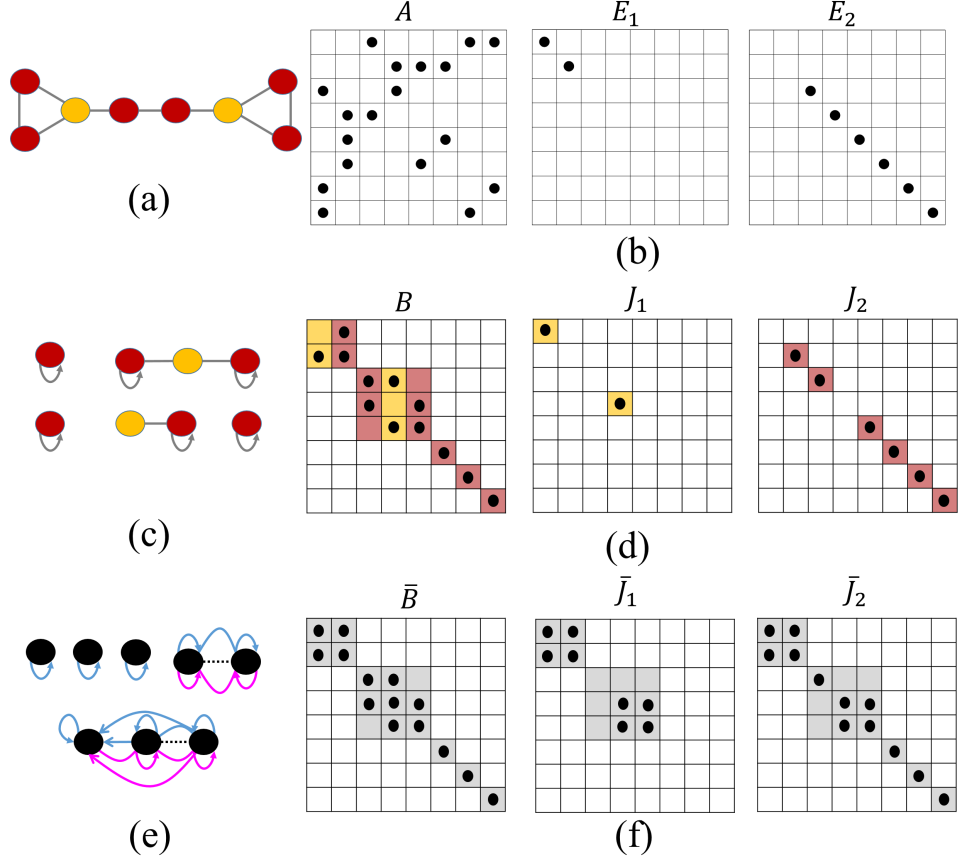


FIG. 3. (a) An $N = 8$ -dimensional network with $C = 2$ equitable clusters. Nodes are color-coded according to the clusters to which they belong. (b) The adjacency matrix of the network (A) and the two cluster indicator matrices ((E_1, E_2)) are graphically shown, in which a nonzero entry is indicated as a black dot. (c) and (e) show the quotient and transverse sub-networks after application of the SBD transformation T and \tilde{T} , respectively. Subnetwork nodes are colored based on the cluster to which they are associated. Black nodes indicate that they are not associated with only one cluster. In (e) connections with different colors represent coupling through the \bar{B} subnetwork and the \bar{J}_i subnetworks. (d) The set of matrices $\{B, J_1, J_2\}$ and (f) the set of matrices $\{\bar{B}, \bar{J}_1, \bar{J}_2\}$ obtained by using the transformation T and \tilde{T} , respectively. The background color of each matrix entry indicates the cluster about which the dynamics is linearized. A gray background color indicates that the dynamics is linearized about multiple clusters.

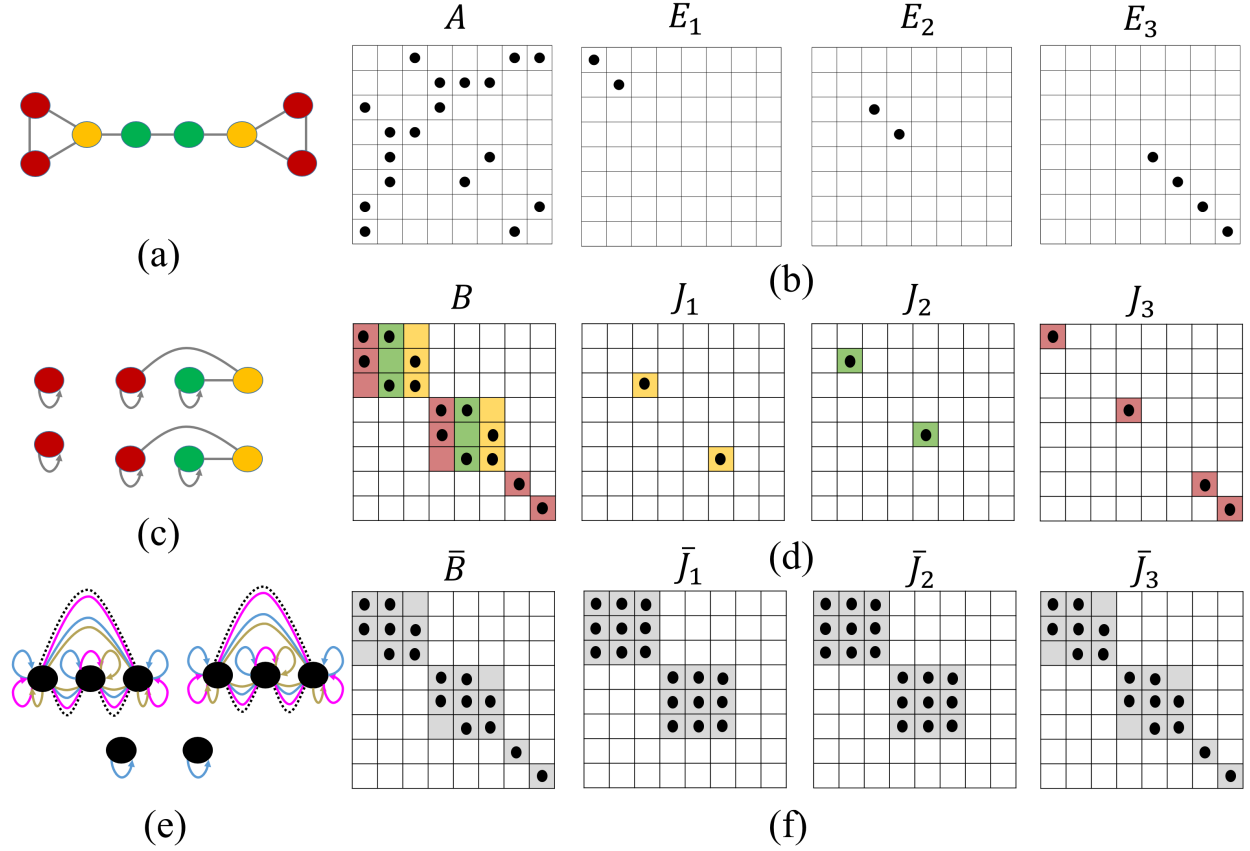


FIG. 4. (a) An $N = 8$ -dimensional network with $C = 3$ orbital clusters. Nodes are color-coded according to the clusters to which they belong. (b) The adjacency matrix of the network (A) and the three cluster indicator matrices ((E_1, E_2, E_3)) are graphically shown, in which a nonzero entry is indicated as a black dot. (c) and (e) show the quotient and transverse sub-networks after application of the SBD transformation T and \tilde{T} , respectively. Subnetwork nodes are colored based on the cluster to which they are associated. Black nodes indicate that they are not associated with only one cluster. In (e) connections with different colors represent coupling through the \bar{B} subnetwork and the \bar{J}_i subnetworks. (d) The set of matrices $\{B, J_1, J_2, J_3\}$ and (f) the set of matrices $\{\bar{B}, \bar{J}_1, \bar{J}_2, \bar{J}_3\}$ obtained by using the transformation T and \tilde{T} , respectively. The background color of each matrix entry indicates the cluster about which the dynamics is linearized. A gray background color indicates that the dynamics is linearized about multiple clusters.

V. REAL NETWORKS ANALYSIS

The ultimate goal of the study of stability of network cluster synchronization is to gain better understanding of real networks of interest. In particular, given a real network and a dynamics on its nodes, one would like to know which patterns of cluster synchronization are possible for that network and how stable those patterns are. It is thus important to consider application of the algorithm developed in this paper to real network topologies.

In Table I we apply both transformation T and \tilde{T} to block diagonalize the adjacency matrices of several real networks from the literature. For each network dataset, we include information on the number of nodes N , the number of edges E , the number of nontrivial clusters N_{ntc} (clusters with more than one node²²), the size of the largest equitable cluster $\max(|n_c|)$ and the average runtime over 10 numerical runs for calculation of the transformation matrices T and \tilde{T} (method from³²). All these networks are connected, undirected and unweighted (only the giant component was considered in the case of networks that are not connected.) For all the networks we have analyzed, the two transformation matrices T and \tilde{T} produced equivalent SBD decompositions, with the same number of blocks and of the same sizes. However, the computation time of our algorithm was (up to six times) faster. It was previously shown that the code proposed in³² is faster than the other codes proposed in Refs.^{18,22}(see Fig. 2 of Ref.³²). Therefore, we only compare the run-time of our code with that of³²

VI. CONCLUSIONS

In this paper we have studied cluster synchronization of networks and proposed a canonical transformation for simultaneous block diagonalization of matrices that we use to study stability of the cluster synchronous (CS) solution. Our approach presents several advantages as it allows us to: (1) decouple the stability problem into blocks of minimal dimensionality, while preserving physically meaningful information; (2) study stability of the CS solution for both the cases of orbital and equitable partitions of the network nodes and (3) obtain a parametrization of the problem in a minimal number of parameters.

When applied to several real network topologies, our algorithm is faster than the one

TABLE I. Real networks analysis. N is the number of nodes, E the number of edges, N_{ntc} is the number of nontrivial clusters, $\max(|n_c|)$ is the size of the largest equitable cluster. We include the average runtime in seconds for calculation of the transformation matrix T and of the transformation matrix \tilde{T} using the code from³².

Name	N	E	N_{ntc}	$\max(n_c)$	Average Runtime for \tilde{T} ³²	Average Runtime for T
ca-netscience: Scientist Collaboration Network ²⁴	379	914	70	6	25.0745	6.4077
Chilean Power Grid Network ^{4,11}	218	527	29	7	2.9198	1.9107
Power Grid Network of Western Germany ¹⁹	491	665	43	5	41.7946	14.4780
Metabolic Network ²⁴	453	2025	28	4	24.6675	12.6427
Us Airline ¹	332	2126	31	12	11.0195	5.8412
Erdos971 ²⁴	429	1312	20	3	16.92	10.0446
celegans-dir: Biological Network ²⁴	453	2025	28	4	23.5363	12.6916
bio-diseasome: Biological Network ²⁴	516	1188	95	6	90.5763	13.9930
fb-forum: social network ²⁴	899	7036	16	5	171.0608	65.6710

proposed in³² and leads to a decomposition of the stability problem into a number of sub-problems that preserve key physical properties of the original system (such as the ‘color’ of the nodes). The main advantage of our canonical transformation is that it allows a parametrization of the stability problem in a small number of parameters. In particular, we show how the stability analysis for different networks can be studied in terms of these parameters and how changing the coupling strengths of a subset of connections is reflected in ‘localized’ variations of these parameters. With this paper, we provide a link to our code, which we hope will be used in conjunction with codes by other groups, such as e.g.,¹⁵ and³².

VII. SUPPLEMENTARY MATERIAL

In the supplementary material, we present other two examples of networks. The first example is a network with $N = 6$ nodes. The second example with $N = 10$ nodes is from²⁷

and has different orbital and equitable cluster partitions. For both the case of the orbital and of the equitable partition, we obtain the same decomposition in blocks previously found in Ref.²⁷.

ACKNOWLEDGEMENT

The authors thank Galen Novello for insightful conversations on the subject of $*$ -algebra.

AUTHOR DECLARATIONS

The authors have no conflicts to disclose.

DATA AVAILABILITY

The data that supports the findings of this study are available within the article.

CODE AVAILABILITY

The MATLAB code to compute the simultaneous block diagonalizations for the cluster synchronization examples shown in this paper can be accessed from its [Github repo](#).

REFERENCES

- ¹Batagelj, V. and Mrvar, A., “Pajek datasets,” (2006).
- ²Belykh, I. and Hasler, M., “Mesoscale and clusters of synchrony in networks of bursting neurons,” *Chaos: An Interdisciplinary Journal of Nonlinear Science* **21**, 016106 (2011).
- ³Belykh, V. N., Osipov, G. V., Petrov, V. S., Suykens, J. A., and Vandewalle, J., “Cluster synchronization in oscillatory networks,” *Chaos: An Interdisciplinary Journal of Nonlinear Science* **18**, 037106 (2008).
- ⁴Bhatta, K., Hayat, M. M., and Sorrentino, F., “Modal decomposition of the linear swing equation in networks with symmetries,” *IEEE Transactions on Network Science and Engineering* (2021).

- ⁵Dahms, T., Lehnert, J., and Schöll, E., “Cluster and group synchronization in delay-coupled networks,” *Physical Review E* **86**, 016202 (2012).
- ⁶Della Rossa, F., Pecora, L., Blaha, K., Shirin, A., Klickstein, I., and Sorrentino, F., “Symmetries and cluster synchronization in multilayer networks,” *Nature communications* **11**, 1–17 (2020).
- ⁷Fu, C., Lin, W., Huang, L., and Wang, X., “Synchronization transition in networked chaotic oscillators: The viewpoint from partial synchronization,” *Physical Review E* **89**, 052908 (2014).
- ⁸Golubitsky, M. and Stewart, I., “Synchrony versus symmetry in coupled cells,” in *EQUAD-*IFF* 2003* (World Scientific, 2005) pp. 13–24.
- ⁹Irving, D. and Sorrentino, F., “Synchronization of dynamical hypernetworks: Dimensionality reduction through simultaneous block-diagonalization of matrices,” *Physical Review E* **86**, 056102 (2012).
- ¹⁰Kanter, I., Kopelowitz, E., Vardi, R., Zigzag, M., Kinzel, W., Abeles, M., and Cohen, D., “Nonlocal mechanism for cluster synchronization in neural circuits,” *EPL (Europhysics Letters)* **93**, 66001 (2011).
- ¹¹Kim, H., Olave-Rojas, D., Álvarez-Miranda, E., and Son, S.-W., “In-depth data on the network structure and hourly activity of the central chilean power grid,” *Scientific data* **5**, 1–10 (2018).
- ¹²Klickstein, I., Pecora, L., and Sorrentino, F., “Symmetry induced group consensus,” *Chaos: An Interdisciplinary Journal of Nonlinear Science* **29**, 073101 (2019).
- ¹³Kudose, S., “Equitable partitions and orbit partitions,” *Acta Mathematica Sinica* , 1–9 (2009).
- ¹⁴Lodi, M., Sorrentino, F., and Storace, M., “One-way dependent clusters and stability of cluster synchronization in directed networks,” *Nature Communications* **12** (2021).
- ¹⁵Maehara, T., “Error-controlled simultaneous block-diagonalization algorithm,” <http://misojiro.t.u-tokyo.ac.jp/~maehara/commdec/index.html> (2012).
- ¹⁶Maehara, T. and Murota, K., “Error-controlling algorithm for simultaneous block-diagonalization and its application to independent component analysis,” *JSIAM Letters* **2**, 131–134 (2010).
- ¹⁷Maehara, T. and Murota, K., “A numerical algorithm for block-diagonal decomposition of matrix *-algebras with general irreducible components,” *Japan journal of industrial and*

- applied mathematics **27**, 263–293 (2010).
- ¹⁸Maehara, T. and Murota, K., “Algorithm for error-controlled simultaneous block-diagonalization of matrices,” *SIAM Journal on Matrix Analysis and Applications* **32**, 605–620 (2011).
- ¹⁹Matke, C., Medjroubi, W., and Kleinhans, D., “SciGRID - An Open Source Reference Model for the European Transmission Network (v0.2),” (2016).
- ²⁰Nicosia, V., Valencia, M., Chavez, M., Díaz-Guilera, A., and Latora, V., “Remote synchronization reveals network symmetries and functional modules,” *Physical review letters* **110**, 174102 (2013).
- ²¹Pecora, L. and Carroll, T., “Master stability functions for synchronized coupled systems,” *Phys. Rev. Lett.* **80**, 2109–2112 (1998).
- ²²Pecora, L. M., Sorrentino, F., Hagerstrom, A. M., Murphy, T. E., and Roy, R., “Cluster synchronization and isolated desynchronization in complex networks with symmetries,” *Nature communications* **5**, 1–8 (2014).
- ²³Rosin, D. P., Rontani, D., Gauthier, D. J., and Schöll, E., “Control of synchronization patterns in neural-like boolean networks,” *Physical review letters* **110**, 104102 (2013).
- ²⁴Rossi, R. A. and Ahmed, N. K., “The network data repository with interactive graph analytics and visualization,” in *Proceedings of the Twenty-Ninth AAAI Conference on Artificial Intelligence* (2015).
- ²⁵Sánchez-García, R. J., “Exploiting symmetry in network analysis,” *Communications Physics* **3**, 1–15 (2020).
- ²⁶Schaub, M. T., O’Clery, N., Billeh, Y. N., Delvenne, J.-C., Lambiotte, R., and Barahona, M., “Graph partitions and cluster synchronization in networks of oscillators,” *Chaos: An Interdisciplinary Journal of Nonlinear Science* **26**, 094821 (2016).
- ²⁷Siddique, A. B., Pecora, L., Hart, J. D., and Sorrentino, F., “Symmetry-and input-cluster synchronization in networks,” *Physical Review E* **97**, 042217 (2018).
- ²⁸Sorrentino, F. and Ott, E., “Network synchronization of groups,” *Phys. Rev. E* **76**, 056114 (2007).
- ²⁹Sorrentino, F., Pecora, L. M., Hagerstrom, A. M., Murphy, T. E., and Roy, R., “Complete characterization of stability of cluster synchronization in complex dynamical networks,” *Science Advances* **2** (2016).
- ³⁰Tinkham, M., *Group theory and quantum mechanics* (Courier Corporation, 2003).

- ³¹Williams, C. R., Murphy, T. E., Roy, R., Sorrentino, F., Dahms, T., and Schöll, E., “Experimental observations of group synchrony in a system of chaotic optoelectronic oscillators,” *Physical review letters* **110**, 064104 (2013).
- ³²Zhang, Y. and Motter, A. E., “Symmetry-independent stability analysis of synchronization patterns,” *SIAM Review* **62**, 817–836 (2020).

Supplementary Material of the paper Cluster Synchronization of Networks via a Canonical Transformation for Simultaneous Block Diagonalization of Matrices

Shirin Panahi, Isaac Klickstein, and Francesco Sorrentino*
Mechanical Engineering Department, University of New Mexico, Albuquerque, NM 87131

I. NOTE 1

Figure 1 (a) shows another example of a network with 6 nodes and 3 clusters. The nodes with the same color belong to the same cluster.

The equitable partitioning of the network shown in Fig. 1 is equivalent to the orbital partitioning of the network using

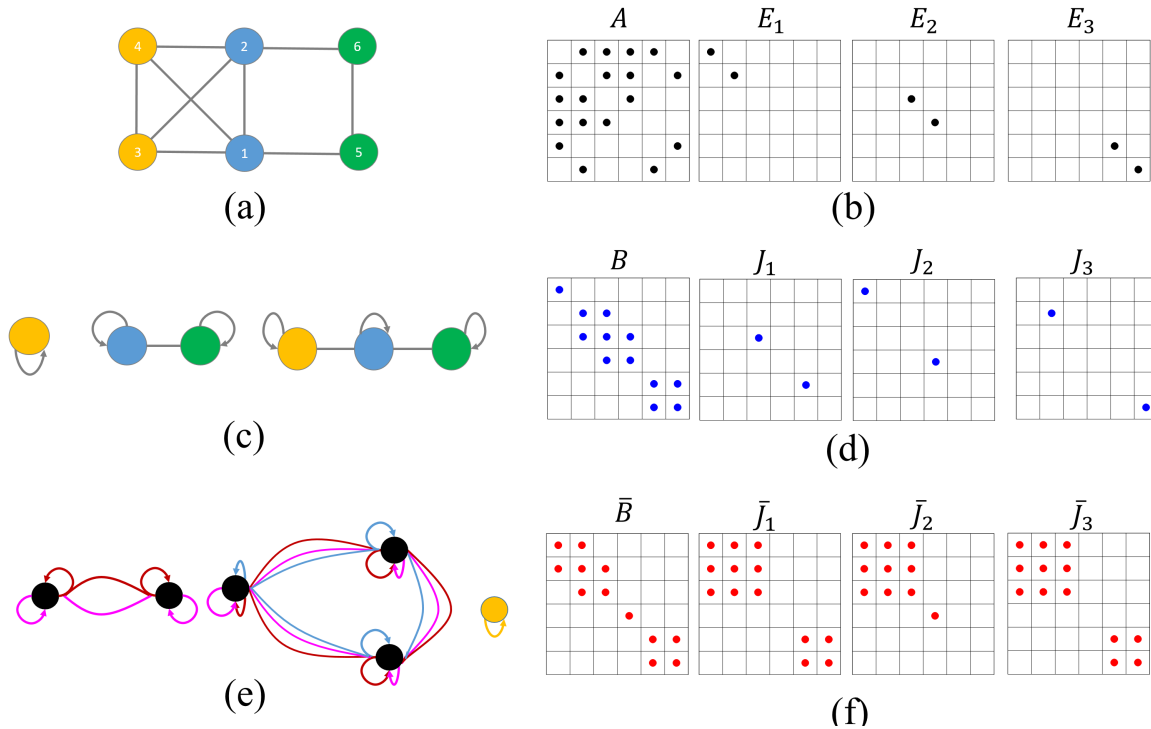


FIG. 1: (a) An 6-dimensional network with 3 clusters. Nodes are color-coded according to the clusters they belong to. (b) The adjacency matrix of the network and three cluster indicator matrices are graphically shown in which a nonzero entry is indicated as a black dot. (c) and (e) Quotient and transverse sub-networks after application of the SBD transformation T and \tilde{T} , respectively. (d) and (f) The transformed version of matrices shown in panel (b) using transformation T and \tilde{T} , respectively. It can be seen that the SBD transformation T is a canonical transformation while \tilde{T} is a non-canonical SBD transformation.

group theory and the network's topological symmetries. In contrast, the network investigated in [?] the equitable and orbital partitioning of the network leads to the two different clusters. Figure 2 (a) shows the 10-dimensional network with 2 equitable clusters. The application of the T and \tilde{T} SBD transformation is shown in Fig. 2 panel (d) and (f), respectively. The same 10-dimensional network of Fig. 2 but with orbital partitioning is shown in Fig. 3 (a). The results shown in panel (d) of the Figs. 2 and 3 show that the application of the SBD transformation proposed in the Sec. IIIA of the main text coincide with the results presented in [?].

*Electronic address: fsorrent@unm.edu

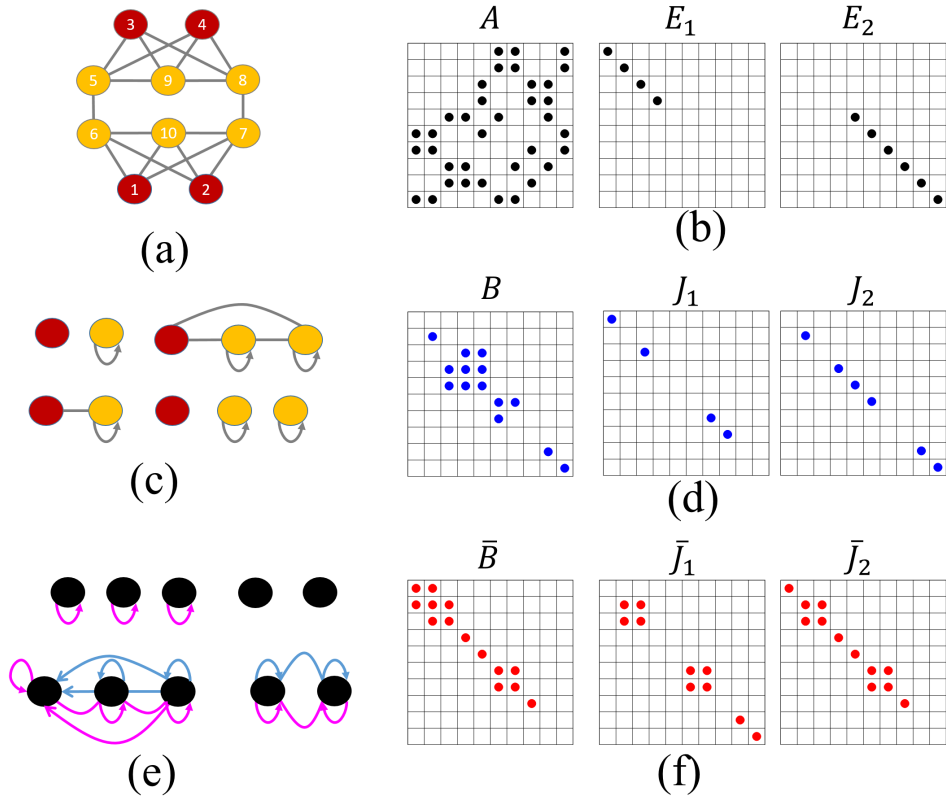


FIG. 2: (a) An $N = 10$ -dimensional network with $C = 2$ equitable clusters. Nodes are color-coded according to the clusters they belong to. (b) The adjacency matrix of the network (A) and the two cluster indicator matrices ((E_1, E_2)) are graphically shown, in which a nonzero entry is indicated as a black dot. (c) and (e) show the quotient and transverse sub-networks after application of the SBD transformation T and \tilde{T} , respectively. Subnetwork nodes are colored based on the cluster they are associated to. Black nodes indicate that they are not associated with only one cluster. In (e) connections with different colors represent coupling through the \bar{B} subnetwork and the \bar{J}_i subnetworks. (d) The set of matrices $\{B, J_1, J_2\}$ and (f) the set of matrices $\{\bar{B}, \bar{J}_1, \bar{J}_2\}$ obtained by using the transformation T and \tilde{T} , respectively. The background shade color of each matrix entry indicates the cluster about which the dynamics is linearized. A gray background shade color indicates that the dynamics is linearized about multiple clusters.

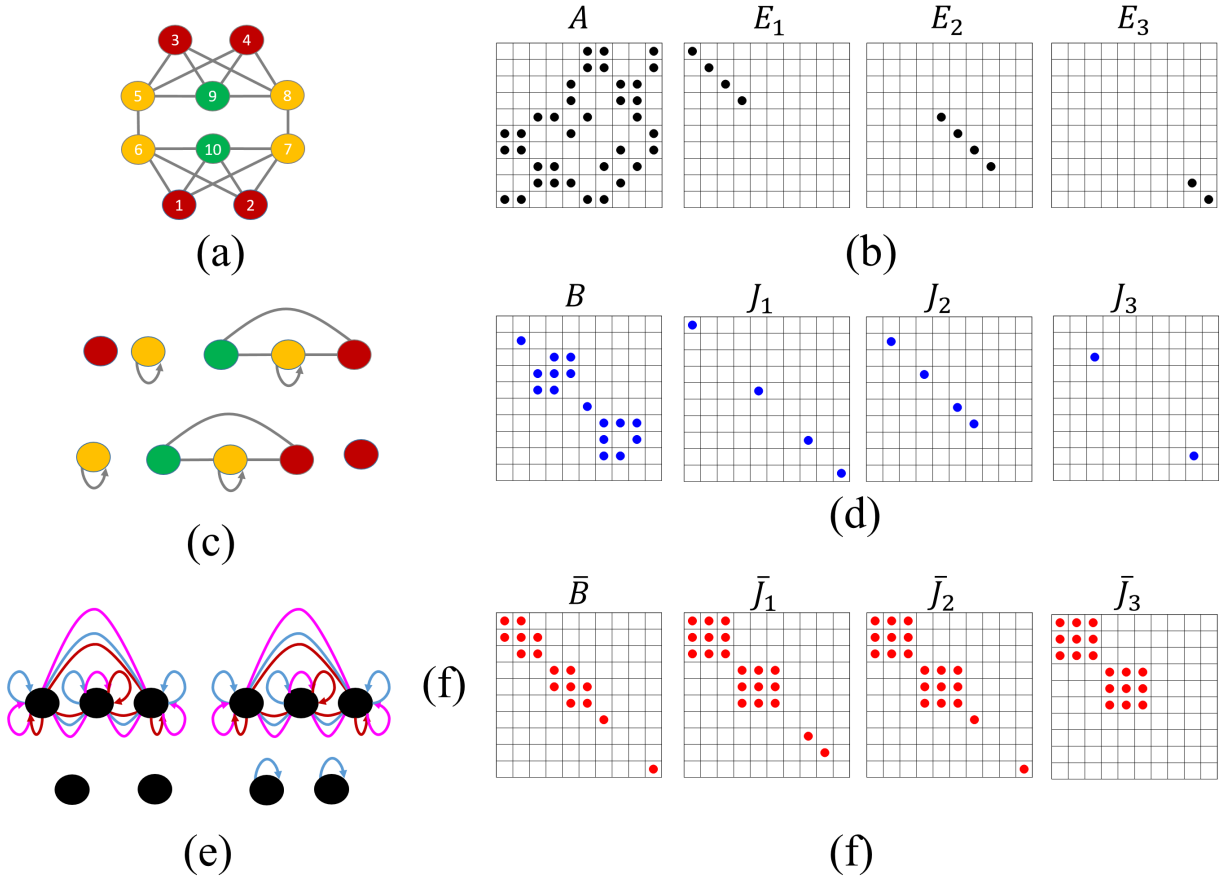


FIG. 3: (a) An $N = 10$ -dimensional network with $C = 3$ equitable clusters. Nodes are color-coded according to the clusters they belong to. (b) The adjacency matrix of the network (A) and the two cluster indicator matrices (E_1, E_2, E_3) are graphically shown, in which a nonzero entry is indicated as a black dot. (c) and (e) show the quotient and transverse sub-networks after application of the SBD transformation T and \tilde{T} , respectively. Subnetwork nodes are colored based on the cluster they are associated to. Black nodes indicate that they are not associated with only one cluster. In (e) connections with different colors represent coupling through the \bar{B} subnetwork and the \bar{J}_i subnetworks. (d) The set of matrices $\{B, J_1, J_2, J_3\}$ and (f) the set of matrices $\{\bar{B}, \bar{J}_1, \bar{J}_2, \bar{J}_3\}$ obtained by using the transformation T and \tilde{T} , respectively. The background shade color of each matrix entry indicates the cluster about which the dynamics is linearized. A gray background shade color indicates that the dynamics is linearized about multiple clusters.